

Tuning the interactions between electron spins in fullerene-based triad systems

Maria A. Lebedeva¹, Thomas W. Chamberlain¹, E. Stephen Davies¹,
Bradley E. Thomas¹, Martin Schröder¹ and Andrei N. Khlobystov^{*1,2}

Full Research Paper

Open Access

Address:

¹School of Chemistry, University of Nottingham, Nottingham, NG7 2RD, UK and ²Nottingham Nanoscience & Nanotechnology Centre, University of Nottingham, University Park, Nottingham, NG7 2RD, UK

Email:

Andrei N. Khlobystov* - andrei.khlobystov@nottingham.ac.uk

* Corresponding author

Keywords:

carbon nanomaterials; electrochemistry; EPR; fullerene dimers; fullerene triads; spin–spin interactions

Beilstein J. Org. Chem. **2014**, *10*, 332–343.

doi:10.3762/bjoc.10.31

Received: 25 September 2013

Accepted: 06 January 2014

Published: 05 February 2014

This article is part of the Thematic Series "Functionalized carbon-nanomaterials".

Guest Editor: A. Krueger

© 2014 Lebedeva et al; licensee Beilstein-Institut.
License and terms: see end of document.

Abstract

A series of six fullerene–linker–fullerene triads have been prepared by the stepwise addition of the fullerene cages to bridging moieties thus allowing the systematic variation of fullerene cage (C_{60} or C_{70}) and linker (oxalate, acetate or terephthalate) and enabling precise control over the inter-fullerene separation. The fullerene triads exhibit good solubility in common organic solvents, have linear geometries and are diastereomerically pure. Cyclic voltammetric measurements demonstrate the excellent electron accepting capacity of all triads, with up to 6 electrons taken up per molecule in the potential range between -2.3 and 0.2 V (vs Fc^+/Fc). No significant electronic interactions between fullerene cages are observed in the ground state indicating that the individual properties of each C_{60} or C_{70} cage are retained within the triads. The electron–electron interactions in the electrochemically generated dianions of these triads, with one electron per fullerene cage were studied by EPR spectroscopy. The nature of electron–electron coupling observed at 77 K can be described as an equilibrium between doublet and triplet state biradicals which depends on the inter-fullerene spacing. The shorter oxalate-bridged triads exhibit stronger spin–spin coupling with triplet character, while in the longer terephthalate-bridged triads the intramolecular spin–spin coupling is significantly reduced.

Introduction

Fabricating molecular systems that are capable of storing one or more unpaired electrons is essential for the development of molecular spintronics and electron-spin-based quantum computing. Endohedral fullerenes are compounds that contain a heteroatom trapped inside the fullerene cage and are able to

support the formation of stable radical materials [1]. They can also show interesting properties such as magnetism, and photoactivity and are thermally and chemically stable. Their ability to form well-ordered 1D arrays makes them leading candidate materials for the study of polyfunctional materials.

For example, significant effort has been directed into incorporating N@C₆₀ molecules into quantum computing devices [2]. Incorporating a second radical centre into these molecules, in addition to the endohedral atom, introduces a mechanism to control the magnetic properties of the resulting materials. This is essential for the recording, storing and read-out processes performed in spin-based quantum information processing using nanoscale molecular architectures [3]. This has been achieved recently within a copper porphyrin–N@C₆₀ dyad [4] and several types of N@C₆₀–N@C₆₀ molecules [5–7]. However the application of these systems is limited due to a number of synthetic challenges associated with the preparation and purification of endohedral fullerenes [8]. This notwithstanding, fullerene cages are excellent electron acceptors and can support up to six electrons per fullerene cage to form species containing one or more unpaired electrons, in which overall charge and the spin state can be controlled precisely by applied potential [9]. In addition, combining two fullerene cages within the same molecule increases the total spin-carrying capacity and introduces a mechanism of spin-tuning while retaining the intrinsic properties of each of the fullerene cages [10]. The synthesis of such fullerene–bridge–fullerene triads, though not straightforward, has been reported [11], the simplest involving species where the fullerene cages are connected directly by a C–C bond [12], a bridging O-atom [13], or by a transition metal atom [14]. A variety of more complex triads have since evolved in which the fullerene molecules are connected using optically or electrochemically active spacers [15]. The choice of linker in triad systems is crucial as it has a significant impact on the properties of the resulting arrays [16]. As the strength of dipolar coupling between unpaired electrons decreases as a function of r^{-3} , where r is the average distance between unpaired electrons, the strength of any electron–electron interactions in fullerene triads rapidly decreases with increasing distance between fullerene cages [17]. Thus, the ability to control the inter-fullerene separation is crucial in fabricating systems in which specific interactions between multiple unpaired electrons are targeted.

The shape of the fullerene containing molecule is also very important. 1D and 2D ordering is a critical factor in the design of molecular electronics. For example, linear molecules can be ordered readily into 1D arrays using carbon nanotubes as templates [18] and are therefore advantageous compared to non-linear or branched molecules for which 1D packing arrangements are inhibited. In addition, solubility can also be a significant issue as fullerene triads tend to show poor solubility [19]. The majority of fullerene triads reported to date are either synthesised via complicated non-scalable synthetic procedures, which makes controlling the fullerene–fullerene distance difficult, or incorporate bulky spacers and solubilising groups

resulting in cumbersome non-linear structures and hence are not ideal for potential applications in molecular electronics and spintronics devices. We recently reported a new general synthetic methodology for the formation of fullerene triads which allows the introduction of fullerene cages in a stepwise fashion and thus allows the length of the spacer to be adjusted [20]. We report herein the preparation of six different fullerene–linker–fullerene triads in which both the length of the linker and the nature of the fullerene cage are systematically varied, and we explore their spin-carrying and spin-tuning capacity in reduced states using electrochemical techniques and electron paramagnetic resonance (EPR) spectroscopy.

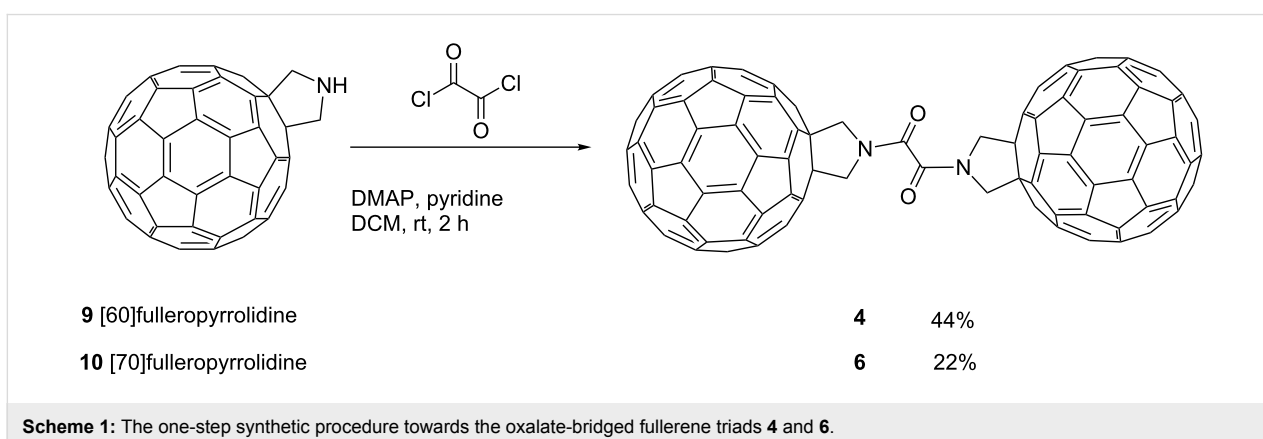
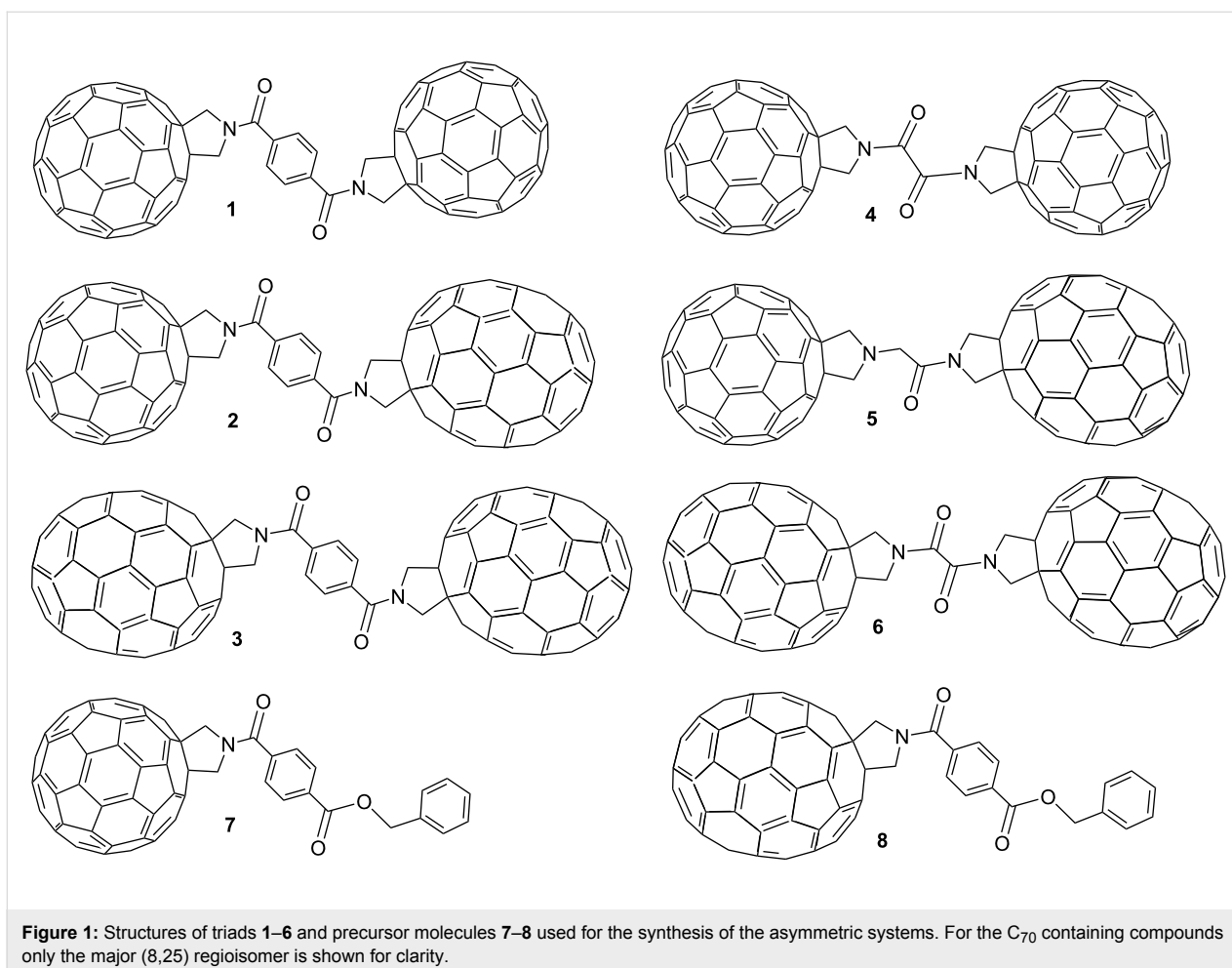
Results and Discussion

Synthesis of the fullerene triads

This study aimed to vary the fullerene–fullerene separation and the nature of the fullerene cages resulting in the preparation of six fullerene–linker–fullerene (triad) compounds (Figure 1). The fullerenes were functionalised via Prato reaction chemistry forming a pyrrolidine ring across the [6.6] bond of the cage [21]. The resulting pyrrolidine functionalised fullerenes are known to be electrochemically stable and can be readily linked together via the N atom to form linear and diastereomerically pure triads. The choice of linker was determined by the target fullerene–fullerene separation in the product, and terephthalate and oxalate bridges were chosen as they possess similar chemical properties but differ significantly in size. The distance between the centres of the corresponding fullerene cages in the terephthalate bridged triads (compounds **1–3**) was estimated to be 16–20 Å depending on the conformation of the molecule (see Figure S4, Supporting Information File 1), whereas the oxalate (compounds **4** and **6**) or acetate (compound **5**) bridged triads have significantly shorter separations (12–15 Å). Functionalised fullerenes **7** and **8**, which are precursors in the synthesis of triads **1–3**, were utilised as control compounds in the electrochemical studies and to aid the assignment of redox processes in the triad species.

The triads **1–3** were synthesised in five steps by functionalisation of each fullerene cage using the Prato reaction, addition of the terephthalate spacer to the fulleropyrrolidine unit and subsequent coupling of two fullerene moieties [20]. The oxalate or acetate bridged triads **4–6** were prepared using a similar strategy. To link the two C₆₀ or two C₇₀ fullerene cages with the oxalate spacer (compounds **4** and **6**) a one-step procedure was used in which the corresponding fulleropyrrolidine was treated with an excess of oxalyl chloride in the presence of 4-dimethylaminopyridine (DMAP) and pyridine (Scheme 1).

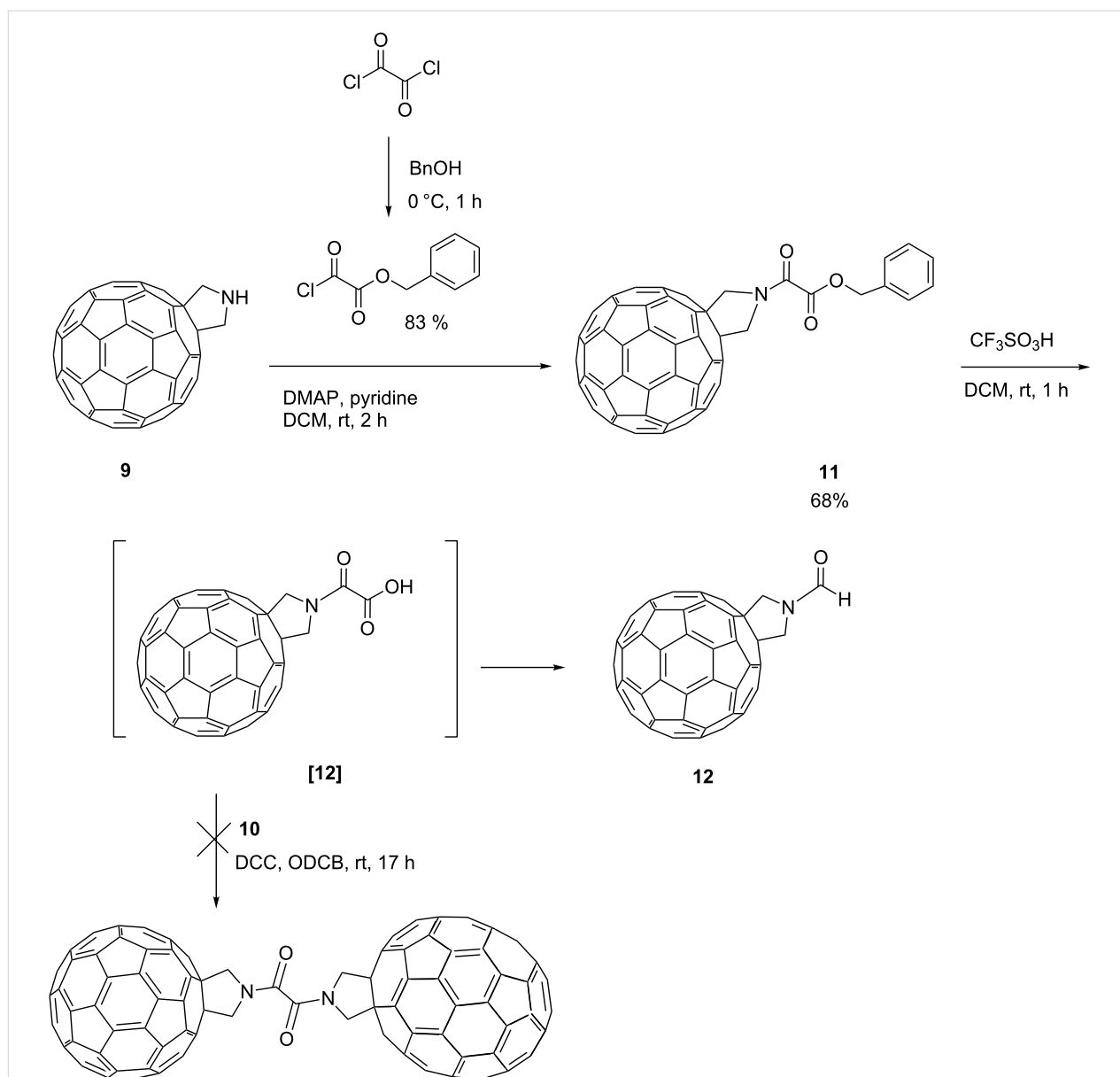
Oxalate bridged triads **4** and **6** were obtained in moderate yields and displayed physical and spectroscopic properties very



similar to those of terephthalate bridged triads 1–3, including good solubility in organic solvents such as CS₂ and *o*-dichlorobenzene (ODCB).

To link the C₆₀ and C₇₀ fulleropyrrolidines within asymmetric triads with an oxalate spacer we attempted a similar stepwise approach as reported for compounds 1–3 (Scheme 2).

Oxalic acid monobenzyl ester monochloride was prepared by equimolar reaction of oxalyl chloride and benzyl alcohol [22] and was reacted with [60]fulleropyrrolidine **9** to give the benzyl ester protected compound **11** in 68% yield. Subsequent deprotection of **11** by CF₃SO₃H yielded the insoluble product **12** that precluded characterisation by solution based methods. However, MALDI-MS of **12** showed a molecular ion peak with



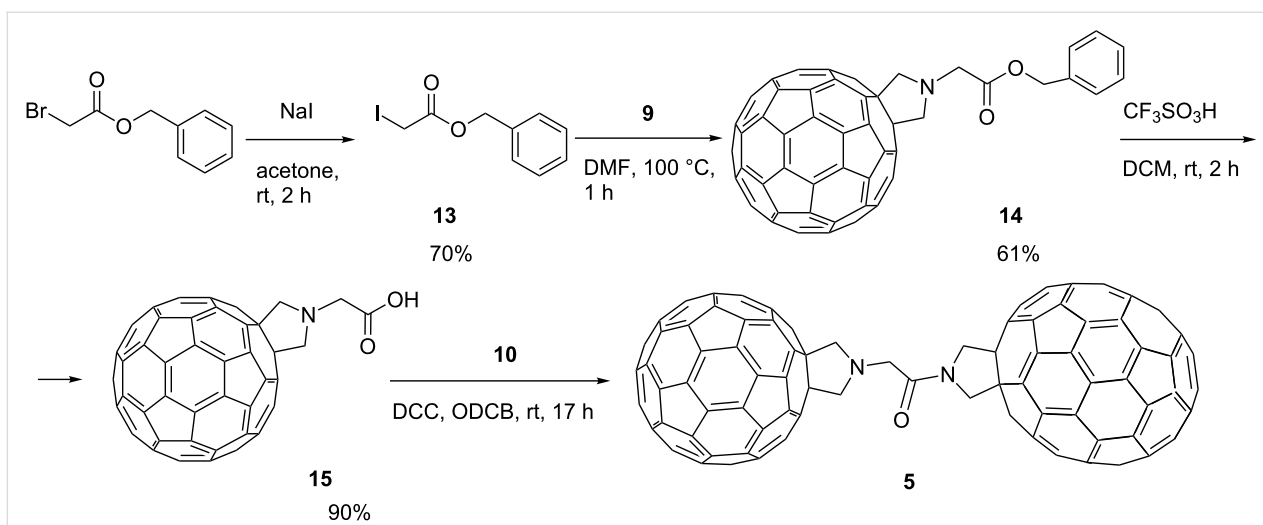
Scheme 2: Attempted synthetic pathway towards the formation of the C₆₀-C₇₀ oxalate bridged fullerene triad allowing the coupling of the fullerene cages in a stepwise fashion.

m/z 791 and the solid state IR spectrum as a pressed disc in KBr indicated only one signal in the carbonyl region characteristic of the amide group (1653 cm⁻¹) and no signal related to the carboxylic group stretch. The desired carboxylic acid compound **[12]** seems to be unstable under acidic conditions and undergoes decarboxylation to form an insoluble amide compound **12**. This reaction under acidic conditions is characteristic of carboxylic acids that contain an electron withdrawing substituent in the α -position [23].

To prevent decarboxylation processes we modified the linker to exclude the electron withdrawing amide group from the α -pos-

ition of the carboxylate functionality, while maintaining an identical inter-fullerene separation in the asymmetric triad when compared with the symmetric analogue (Scheme 3).

The key step in this procedure is the formation of intermediate compound **14** via the nucleophilic substitution of the iodide centre in benzyl 2-iodoacetate [24] (**13**) with [60]fulleropyrrolidine **9** (Scheme 3). Compound **14** is a benzyl ester of an α -amino acid which is stable under acidic conditions. Indeed, deprotection of **14** yielded the desired carboxylic acid **15**. Compound **15** also shows limited solubility, but MALDI-MS (m/z 821) and IR spectroscopy (carbonyl stretch at 1733 cm⁻¹)



Scheme 3: Synthetic pathway to the asymmetric fullerene triad **5** allowing introduction of the fullerene cages in a stepwise fashion.

confirm the assigned structure. The dicyclohexylcarbodiimide (DCC) assisted acid–amine coupling reaction between **15** and [70]fulleropyrrolidine **10** resulted in the formation of the desired asymmetric triad **5**, which displayed physical properties similar to those of **1–4** and **6**.

Electrochemical characterisation of fullerene triads **1–6**

Compounds **1–6** were studied by cyclic voltammetry (CV) as solutions in *o*-dichlorobenzene in order to investigate the sequence of electron additions and possible electronic interactions in these triads.

The cyclic voltammograms recorded for the fullerene triads **1–6** are very similar to those of their monomeric precursors **7** and **8** and do not appear to show interactions between the individual

fullerene cages. This observation is consistent with the lack of an effective electronic communication pathway through the linker groups within the triads (Table 1 and Figure 2).

Each triad molecule **1–6** exhibits a series of reduction processes in a potential range between -0.3 and -2.3 V (vs Fc^+/Fc), some of which are overlapping or appear as shoulders to the main peaks. By comparison with the cyclic voltammetry of the precursor compounds **7** and **8** (Figure S5, Supporting Information File 1), we suggest that this series of reductions corresponds to the addition of up to 3 electrons per fullerene cage (in total 6 electrons per molecule). No oxidation processes were found in the range up to 1.5 V (vs Fc^+/Fc). For triads **1** and **4**, containing C_{60} only, these potentials are similar to those of their precursor **7**. A similar correlation was noted for the C_{70} containing triads **3** and **6** and their precursor **8**. Comparison of **1**

Table 1: Electrochemical data^a for fullerene based compounds **1–8**.

Compound	$E_{1/2}$ red ₁ , V	$E_{1/2}$ red ₂ , V	$E_{1/2}$ red ₃ , V	ΔE , Fc^+/Fc
1	-1.09 (0.16)	-1.47 (0.16)	-2.01 (0.16)	0.17
2	-1.12 (0.10)	-1.48 (0.08)	-1.89 (0.05) -2.02 (0.06)	0.20
3	-1.12 (0.06)	-1.50 (0.08)	-1.89 (0.06)	0.10
4	-1.09 (0.16)	-1.47 (0.16)	-2.01 (0.18)	0.16
5	-1.13 (0.10)	-1.49 (0.10)	-1.89 (0.11) -2.05 (0.10)	0.10
6	-1.10 (0.11)	-1.47 (0.10)	-1.89 (0.11)	0.12
7	-1.11 (0.09)	-1.49 (0.09)	-2.02 (0.08)	0.15
8	-1.15 (0.06)	-1.52 (0.06)	-1.94 (0.06)	0.09

^aPotentials ($E_{1/2} = (E_p^a + E_p^c)/2$) in volt are quoted to the nearest 0.01 V. All potentials are reported against the Fc^+/Fc couple for 0.5 mM solutions in *o*-dichlorobenzene containing 0.2 M $[n\text{-Bu}_4\text{N}][\text{BF}_4]$ as the supporting electrolyte. The anodic/cathodic peak separation ($\Delta E = E_p^a - E_p^c$) is given in brackets where applicable. ΔE for the Fc^+/Fc couple was used as the internal standard.

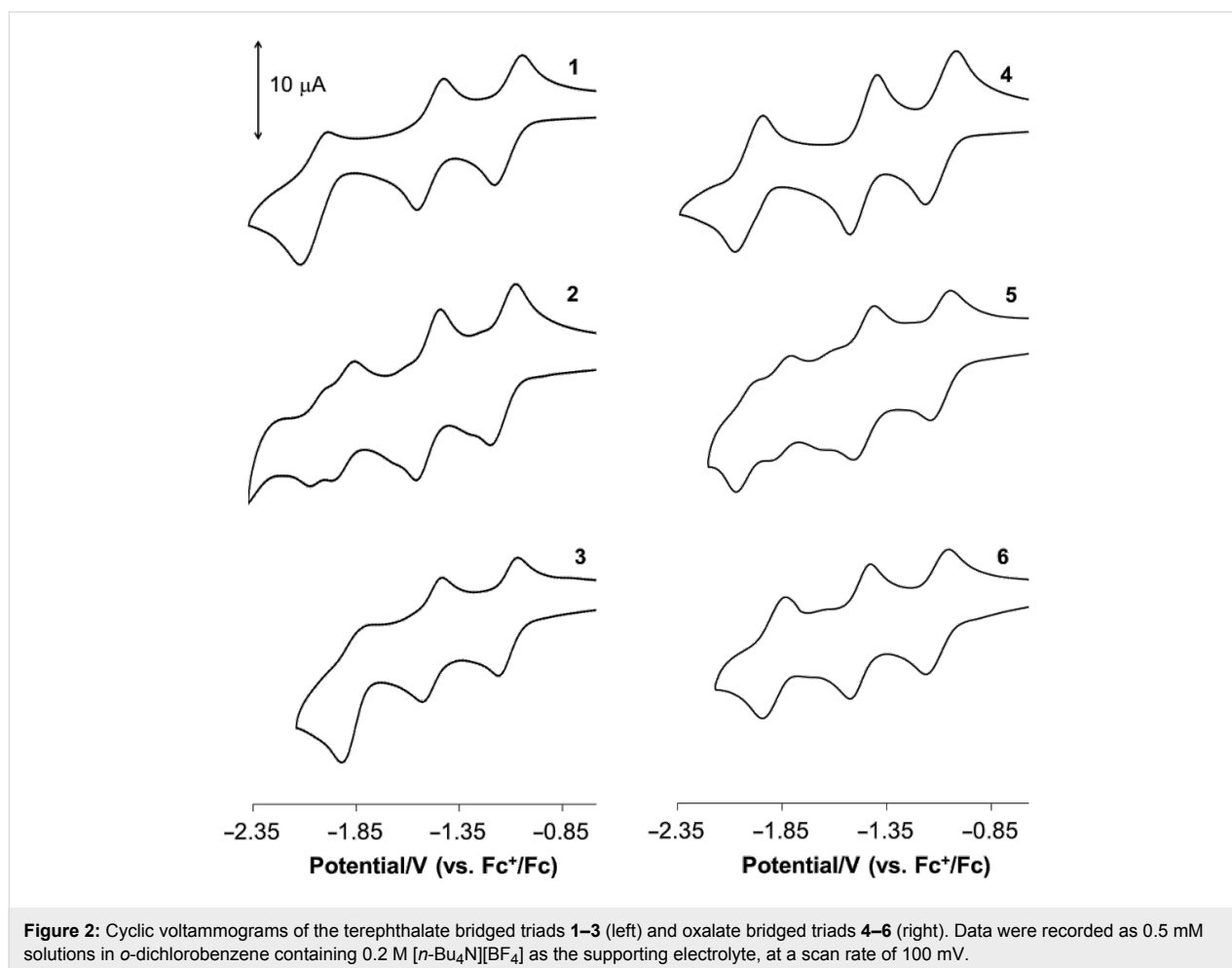


Figure 2: Cyclic voltammograms of the terephthalate bridged triads **1–3** (left) and oxalate bridged triads **4–6** (right). Data were recorded as 0.5 mM solutions in *o*-dichlorobenzene containing 0.2 M [*n*-Bu₄N][BF₄] as the supporting electrolyte, at a scan rate of 100 mV.

with **3**, **4** with **6** and **7** with **8** shows that the first and second reductions of C₆₀, in general, occur at slightly more anodic potentials than those of C₇₀ cages. However beyond the second reduction, C₇₀ is more readily reduced. For **2** and **5**, each containing a mixture of C₆₀ and C₇₀ fullerenes, two well defined reduction couples are observed at $E_{1/2}$ ca. -1.12 and -1.49 V, which we assigned to an overlap of C₆₀/C₇₀-based reductions. These processes are separated by an additional process that appears as a shoulder on the first reduction in **2** and **5** (Figure 2 and Figure S6, Supporting Information File 1). A similar feature is noted to cathodic potential of the second reduction process. For **2** and **5** we associate these features with the generation of a reduced C₇₀ cage in a triad molecule, noting a similar, although less pronounced effect in **3** and **6**, each containing two equivalent C₇₀ cages (see Supporting Information File 1) and an absence of these features in C₆₀ triads, **1** and **4**, and in the C₇₀ containing dyad, **8**. The origin of these effects is unclear and may result from the nature of interaction of the reduced triad with the electrode surface. We note that the first and second reductions on C₇₀ are expected to be slightly more cathodic than those for C₆₀ but comparing

potentials for **7** and **8**, we suggest that this difference alone is too small to explain the position of these features. We note also that **2** and **5** are mixtures of two regioisomers of the pyrrolidine functionalised C₇₀ [19], in a ratio of 6:4 as determined by ¹H NMR spectroscopy (see Experimental section). It is possible that these isomers may interact with the electrode differently.

Based on these results we can confirm that for C₆₀–C₆₀ triad molecules changing the nature and the size of the bridging group has little effect on the nature and potentials of the redox processes. Thus, we conclude that the two C₆₀-fullerene cages in the triads behave independently in the ground state. These results are consistent with other fullerene triad systems in which intramolecular fullerene–fullerene interactions are only observed where fullerene cages are bonded directly [25] or bridged by a transition metal atom [26,27]. For triads containing C₇₀ the results are less clear where additional electrode processes are observed. However we do not attribute these features to intramolecular fullerene–fullerene interactions.

EPR spectroscopic characterisation of the fullerene triads in the reduced state

The electron spin–spin interactions that are crucial for the application of fullerene triads were investigated by EPR spectroscopy as fluid and frozen solutions at room temperature and 77 K, respectively, following electrochemical reduction. Whilst these triads are capable of accepting multiple electrons into each of the fullerene groups, we restrict our discussion to dianionic species in compounds where the electrochemistry is well defined; under these conditions each fullerene cage is reduced by a single electron. We have evaluated the effects of varying the inter-fullerene separation (oxalate bridge vs terephthalate bridge) and the nature of the fullerene (C_{60} vs C_{70}) on the nature of the spin–spin coupling obtained.

The two electron reduced species of **1** and **4** (1^{2-} and 4^{2-}) and the corresponding mono reduced species of their monomeric precursor **7** (7^{1-}) (i.e. one electron per fullerene cage for all species) were obtained by electrochemical reduction at -1.4 V of 0.5 mM solutions of compound in *o*-dichlorobenzene containing $[n\text{-Bu}_4\text{N}][\text{BF}_4]$ as the supporting electrolyte.

Fluid solution EPR spectra of 1^{2-} , 4^{2-} and 7^{1-} (Figure 3) are similar in g value (2.0002, 2.0001 and 2.0000, respectively) but

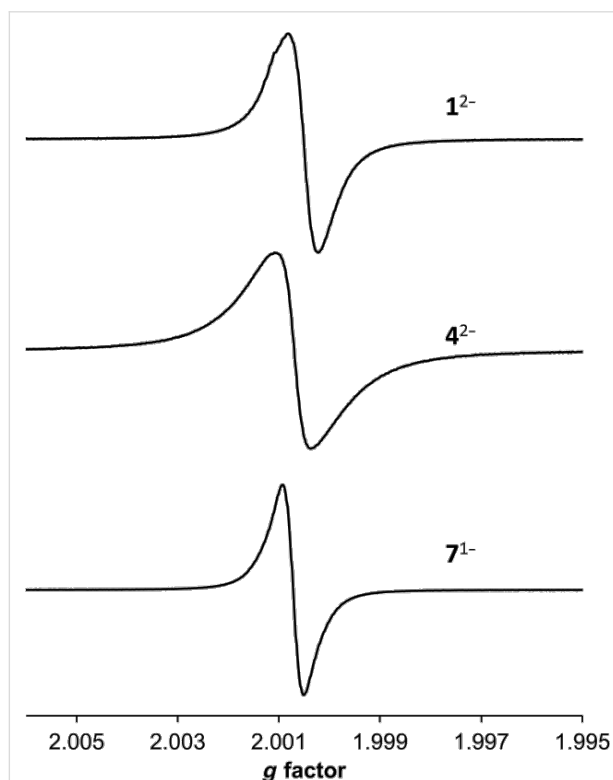


Figure 3: Fluid solution EPR spectra recorded at 297 K for the two electron reduced species of compounds **1** and **4** and the one electron reduced species of **7**.

differ in linewidth (ΔH_{p-p} 1.1, 1.3 and 0.8 G, respectively) and are typical of C_{60} based radical anions [28], confirming that the electrochemically introduced electrons are localised on the fullerene cages.

The EPR spectrum of 4^{2-} in frozen solution recorded at 77 K shows an intense central feature at $g = 2.0001$ (Figure 4a) indicating that the majority of the molecules exist as two independent doublet ($S = 1/2$) radicals and suggesting a small singlet-triplet energy gap [29]. The intramolecular triplet biradical ($S = 1$) of 4^{2-} is also present with a zero-field splitting parameter (D) of 27.8 G (Figure 4a,b). This value is in the same range (26–29 G) as that observed for other triplet biradicals of pyrrolidine-functionalised C_{60} derivatives in C_{60} –bridge– C_{60} triads [15,28] and gives an average distance of 10 Å between the unpaired electrons [16], a distance well within the range predicted by models of **4** (Figure S4b, Supporting Information File 1). The half-field signal corresponding to the triplet state is not observed which is also consistent with previous reports for fulleride based triplets [30]. The presence of an intramolecular triplet would indicate that the distance between the two fulleropyrrolidine units is short enough to allow through-space interaction despite the lack of electronic conjugation between the interacting units. In addition to the intramolecular triplet, a set of inner features is tentatively assigned to an intermolecular (or “powder”) triplet ($D = 7.9$ G) that may result from the aggregation of 4^{2-} molecules in the frozen solution however we do not exclude other possible assignments [31].

The frozen solution EPR spectrum of 1^{2-} displays a central feature at $g = 2.0003$, consistent with that of a doublet biradical (Figure 4c) that is flanked on each side by broad “wings” that we assign to the presence of an intermolecular triplet and give a maximum D value of 9 G which is similar to that observed in the spectrum of 4^{2-} . The same “wings” around the central feature ($g = 2.0000$) have been observed in the EPR spectra of the one electron reduced species of the monomer **7** (Figure S7, Supporting Information File 1) and hence may be explained by intermolecular interactions. Also present are small baseline features (Figure 4d) that may represent the outer features of either an intramolecular or intermolecular triplet. We note similar small baseline features in the spectrum of 7^{1-} ; in this case their assignment to an intramolecular triplet must be excluded. Hence, by changing the linker from oxalate in 4^{2-} to terephthalate in 1^{2-} we have either reduced the interaction of the spin centres or significantly perturbed the formation of an intramolecular triplet biradical.

The EPR spectra of the C_{70} containing compounds 6^{2-} and 8^{1-} (Figure S8, Supporting Information File 1) in fluid solution recorded at room temperature (Figure S8a, Supporting Informa-

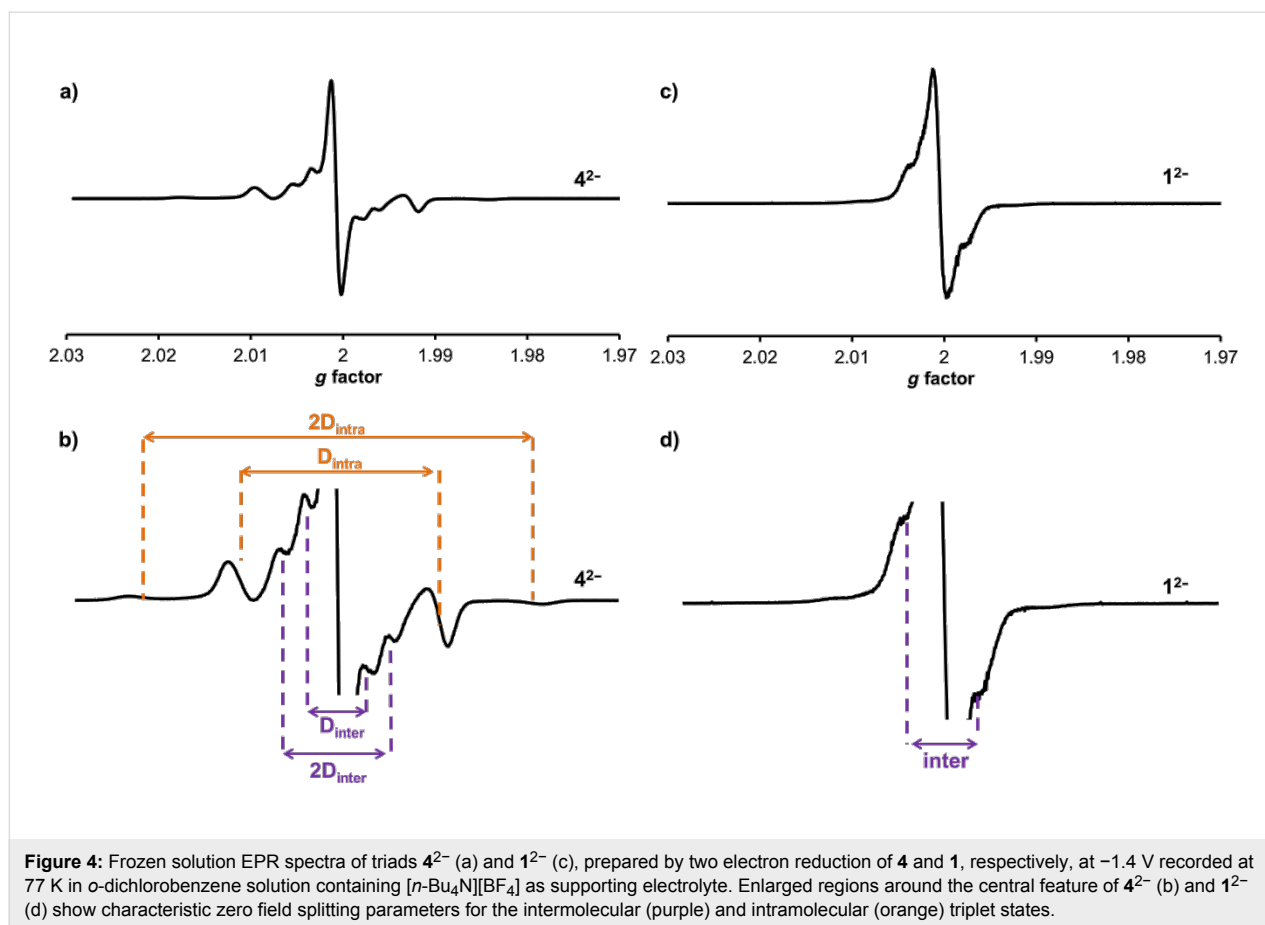


Figure 4: Frozen solution EPR spectra of triads 4^{2-} (a) and 1^{2-} (c), prepared by two electron reduction of **4** and **1**, respectively, at -1.4 V recorded at 77 K in *o*-dichlorobenzene solution containing $[n\text{-Bu}_4\text{N}][\text{BF}_4]$ as supporting electrolyte. Enlarged regions around the central feature of 4^{2-} (b) and 1^{2-} (d) show characteristic zero field splitting parameters for the intermolecular (purple) and intramolecular (orange) triplet states.

tion File 1) and particularly in frozen solution recorded at 77 K (Figure S8b, Supporting Information File 1) are significantly different from those observed for the reduced C_{60} containing compounds. The difference is due to the lower symmetry of the C_{70} (D_{5h} compared to I_h of the C_{60}) which results in an anisotropic spectrum [30]. In addition, due to this asymmetry the spectra are significantly broader which means that any features corresponding to the triplet biradicals will overlap with the main central features and hence are not resolved. This complicates the assignment of the spin states in the C_{70} containing compounds and hence they were not investigated further in this study.

Conclusion

We have developed a synthetic methodology for a range of linear, soluble fullerene triads where the nature of the fullerene cage and the length of the bridge between the cages can be controlled. Cyclic voltammetry measurements demonstrate the high electron accepting capacity of these molecules, which can accept up to six electrons reversibly, but indicate no interactions between the fullerene cages in the ground state of the triads, regardless of the nature of the fullerene (C_{60} or C_{70}) or the length of the bridge (oxalate or terephthalate). The first and

second reduction potentials of C_{60} and C_{70} in the asymmetric triads appear to be indistinguishable, whilst the third reduction of the two fullerene cages is observed as two separate one-electron processes with the reduction potential being slightly less cathodic for the C_{70} cage. EPR spectroscopy measurements of the two electron reduced triads reveal that the nature of the intramolecular electron spin–spin interactions is dependent on the length of the bridge. Specifically, the two electron reduced oxalate bridged triad, where the fullerene cages are separated by a minimum distance of 12 \AA , can exhibit strong intramolecular spin coupling with a D value of 27.8 G . Under the same conditions the triad with the terephthalate bridge, where fullerene cages are separated by a minimum distance of over 16 \AA , does not show similar strong intramolecular spin coupling and may exist mainly as an independent doublet biradical. Our methodology enables precise control of the inter–fullerene separation thus providing a mechanism for controlling the spin properties of fullerene triads which is important for the future development of molecular electronic and spintronic devices.

Experimental

C_{60} (99.5%) and C_{70} (95%) were purchased from SES Research and MER corporation respectively. CH_2Cl_2 was freshly distilled

over CaH_2 before use. All other reagents and solvents were purchased from Aldrich and used without further purification. Compounds **1–3** and **7–10** were synthesised according to previously reported procedure [20]. Infra-red spectra were measured as KBr discs using a Nicolet Avatar 380 FTIR spectrometer over the range $400\text{--}4000\text{ cm}^{-1}$. ^1H and ^{13}C NMR spectra were obtained using Bruker DPX 300, Bruker DPX 400, Bruker AV(III) 400 or Bruker AV(III) 500 spectrometers. Mass spectrometry was carried out using a Bruker microTOF spectrometer and a Bruker ultraFlexIII MALDI–TOF spectrometer using trans-2-[3-(4-*tert*-butylphenyl)-2-methyl-2-propenylidene]malononitrile (DCTB) as supporting matrix. UV–vis spectra were measured using a Lambda 25 Perkin Elmer Spectrometer. EPR spectra were obtained on a Bruker EMX EPR spectrometer.

Cyclic voltammetry

Cyclic voltammetric studies were carried out using an Autolab PGSTAT20 potentiostat, using a three-electrode arrangement in a single compartment cell. A glassy carbon working electrode, a Pt wire secondary electrode and a saturated calomel reference electrode (chemically isolated from the test solution via a bridge tube containing electrolyte solution and fitted with a porous Vycor frit) were used in the cell. Experiments were performed under an atmosphere of argon and in anhydrous solvents. Sample solutions were prepared under an atmosphere of argon using Schlenk line techniques and consisted of a 0.2 M [*n*-Bu₄N][BF₄] solution as the supporting electrolyte and a 0.5 mM solution of the test compound. Redox potentials were referenced vs the Fc^+/Fc couple, which was used as an internal standard. Compensation for internal resistance was not applied.

Bulk electrolysis

Bulk electrolysis experiments at a controlled potential were carried out using a two-compartment cell. A Pt/Rh gauze basket working electrode was separated from a wound Pt/Rh gauze secondary electrode by a glass frit. A saturated calomel electrode was bridged to the test solution through a Vycor frit that was orientated at the centre of the working electrode. The working electrode compartment was fitted with a magnetic stirrer bar and the test solution was stirred rapidly during electrolysis. Each solution contained [*n*-Bu₄N][BF₄] (0.2 M) as the supporting electrolyte and the compound under investigation (5 mL, 0.5 mM) and were prepared using Schlenk line techniques.

Synthesis of the fullerene triads **4–6**

Synthesis of **4**

[60]Fulleropyrrolidine **9** (35 mg, 0.045 mmol) was suspended in freshly distilled CH_2Cl_2 (35 mL) with 4-dimethylaminopyridine (17 mg, 0.139 mmol) and pyridine (0.35 mL), and the reaction

mixture was stirred for 10 min. Oxalyl chloride (0.1 mL, 1.16 mmol) was then added, and the reaction mixture stirred at room temperature for 2 h. On removal of solvent, the resulting residue was dissolved in CS_2 (40 mL) by sonication, and any undissolved material removed by filtration. The filtrate was concentrated and purified by column chromatography (silica gel, *o*-dichlorobenzene/isopropyl alcohol 99.5:0.5) to give the product which was washed with MeOH (30 mL), petroleum ether 40–60 (30 mL) and diethyl ether (30 mL). The resultant solid was dried under vacuum to give the product (16 mg, 44%) as a brown solid. ^1H NMR (400 MHz, 297 K, $\text{CS}_2/\text{CDCl}_3$, δ , ppm) 5.79 (s, 4H, CH_2), 5.69 (s, 4H, CH_2); ^{13}C NMR (125 MHz, 297 K, $\text{CS}_2/\text{CDCl}_3$, δ , ppm) 160.97 (CO), 153.09, 152.74, 147.47, 146.46, 146.44, 146.26, 146.24, 145.80, 145.72, 145.46, 145.43, 145.40, 145.38, 144.59, 144.46, 143.21, 142.83, 142.80, 142.30, 142.23, 142.21, 142.16, 142.07, 142.05, 140.50, 140.40, 135.97, 135.76, 133.02, 130.61, 128.44, 127.69 (sp^2 carbons, 31 environments), 70.85, 69.31, 60.22, 57.07 (sp^3 carbons, 4 environments); MALDI–TOF MS (DCTB/MeCN, m/z): 1580.2 (M^-); IR (KBr, ν , cm^{-1}): 2960 (w), 2922 (w), 1645 (s), 1453 (w), 1328 (m), 1186 (m), 746 (m), 526 (s); UV–vis (CS_2): λ_{max} ($\epsilon \times 10^{-3}/\text{dm}^3\text{ mol}^{-1}\text{ cm}^{-1}$): 703 (0.750), 433 (8.526).

Synthesis of **6**

[70]Fulleropyrrolidine **10** (20 mg, 0.023 mmol) was suspended in CH_2Cl_2 (18 mL), and DMAP (8.7 mg, 0.071 mmol) and pyridine (0.2 mL) were added. The reaction mixture was stirred for 10 min and oxalyl chloride (0.055 mL, 0.64 mmol) was added. The reaction mixture was stirred at room temperature for 2 h, and the solvent was then removed. The resulting residue dissolved in CS_2 (40 mL) by sonication, and the undissolved material removed by filtration. The filtrate was concentrated and purified by column chromatography (silica gel, *o*-dichlorobenzene/isopropyl alcohol 99.5:0.5) to give the product which was washed with MeOH (30 mL) and petroleum ether 40–60 (30 mL). The resultant material was dried under vacuum to give the product (9 mg, 22%) as a brown solid. ^1H NMR (400 MHz, 297 K, $\text{CS}_2/\text{CDCl}_3$, δ , ppm) 5.25–4.36 (m, 8H, CH_2); ^{13}C NMR (125 MHz, 297 K, $\text{CS}_2/\text{CDCl}_3$, δ , ppm) 168.90 (C=O), 167.43 (C=O), 156.55, 156.13, 155.02, 154.96, 154.11, 152.17, 151.56, 151.42, 151.35, 151.07, 151.01, 151.00, 150.96, 150.94, 150.78, 150.71, 150.41, 150.37, 149.93, 149.89, 149.85, 149.79, 149.47, 149.40, 149.36, 149.31, 149.26, 149.11, 149.07, 149.03, 148.79, 148.45, 148.10, 148.06, 147.88, 147.46, 147.21, 147.10, 147.08, 147.05, 147.00, 146.96, 146.93, 146.64, 146.62, 146.57, 145.84, 145.71, 145.53, 145.41, 145.00, 144.90, 144.84, 144.50, 144.48, 144.23, 144.20, 144.16, 144.12, 144.08, 143.48, 143.43, 143.32, 143.26, 143.18, 143.10, 141.43, 140.32, 140.30, 140.27, 137.28, 133.76, 133.72, 133.68, 132.41, 132.13, 131.38, 131.28, 131.25, 128.40 (sp^2 carbons, 80 environments), 71.84, 69.68, 68.74, 64.10, 62.67, 62.63 (sp^3 carbons, 6 envi-

ronments); MALDI-TOF MS (DCTB/MeCN, m/z): 1820.5; IR (KBr, ν , cm^{-1}): 2932 (m), 2363 (s), 1663 (s, C=O), 1435 (m), 669 (s); UV-vis (CS_2): λ_{max} ($\epsilon \times 10^{-3}/\text{dm}^3 \text{ mol}^{-1} \text{ cm}^{-1}$): 693 (3.74), 556 (20.32), 476 (39.28), 462 (39.60), 411 (48.49).

Synthesis of 5

Compound **15** (16 mg, 0.018 mmol), [70]fulleropyrrolidine **10** (16 mg, 0.019 mmol) and dicyclohexylcarbodiimide (3.9 mg, 0.019 mmol) were suspended in anhydrous *o*-dichlorobenzene (2.7 mL) and stirred at room temperature under an Ar atmosphere for 17 h. The reaction mixture was purified by column chromatography (silica gel, *o*-dichlorobenzene) to afford the product which was washed with MeOH (30 mL) and petroleum ether (30 mL) to give the product (9 mg, 27%) as a dark brown solid. Isomer **a** (see Supporting Information File 1): ^1H NMR (400 MHz, 297 K, $\text{CS}_2/\text{CDCl}_3$, δ , ppm) 5.47 (s, 4H, CH_2), 5.28 (m, 2H, CH_2), 4.77 (s, 2H, CH_2), 4.66 (s, 2H, CH_2); Isomer **b** (see Supporting Information File 1): ^1H NMR (400 MHz, 297 K, $\text{CS}_2/\text{CDCl}_3$, δ , ppm) 5.63 (s, 1H), 4.97 (m, 1H), 4.88 (s, 1H), 4.61 (m, 2H), 4.27 (s, 2H), 4.16 (s, 1H), 4.11 (m, 2H); ^{13}C NMR (125 MHz, 297 K, $\text{CS}_2/\text{CDCl}_3$, δ , ppm) 165.69 (C=O), 155.45, 155.16, 155.07, 154.23, 153.30, 153.19, 151.74, 151.38, 151.21, 151.19, 150.92, 150.79, 150.74, 150.66, 149.91, 149.89, 149.81, 149.36, 149.35, 149.32, 149.24, 149.09, 148.78, 148.44, 148.13, 147.61, 147.41, 147.21, 146.94, 146.36, 146.18, 146.15, 145.94, 145.89, 145.57, 145.40, 145.31, 144.64, 144.60, 143.45, 143.22, 143.07, 142.78, 142.18, 142.03, 140.60, 140.38, 139.15, 137.17, 134.25, 133.75, 132.92 (sp^2 carbons, 52 environments), 74.22, 73.26, 70.50, 68.18, 68.14, 64.51, 63.11 (sp^3 carbons, 7 environments); MALDI-TOF MS (DCTB/MeCN, m/z): 1686.3; IR (KBr, ν , cm^{-1}): 2926 (s), 2365 (s), 1674 (s, C=O), 1433 (m), 1250 (m), 1182 (m), 1119 (m), 671 (w), 527 (m); UV-vis (CS_2): λ_{max} ($\epsilon \times 10^{-3}/\text{dm}^3 \text{ mol}^{-1} \text{ cm}^{-1}$): 693 (2.51), 556 (11.83), 479 (22.00), 456 (22.91), 430 (22.48), 410 (30.38).

Oxalic acid monobenzyl ester monochloride [22]

Oxalyl chloride (1 mL) was cooled to 0 °C, and anhydrous benzyl alcohol (1.4 mL) added dropwise over 15 min. After the addition of the alcohol was completed, the reaction mixture was warmed up to room temperature and stirred for 1.5 h. The resulting mixture was analysed by ^1H and ^{13}C NMR spectroscopy and found to be a mixture of the oxalic acid monobenzyl ester monochloride and the dibenzyl oxalate in a 5:1 molar ratio. The mixture was used in the next step immediately without further purification. ^1H NMR (300 MHz, 297 K, CDCl_3 , δ , ppm) 7.47–7.42 (m, 5H), 7.42–7.38 (m, 1.75 H), 5.38 (s, 2H), 5.32 (s, 0.72 H); ^{13}C NMR (75 MHz, 297 K, CDCl_3 , δ , ppm) 160.95, 157.57, 155.53, 134.18, 133.33, 129.35, 128.91, 128.78, 128.74, 70.38, 68.63.

[60]Fulleropyrrolidine oxalate benzyl ester 11

[60]Fulleropyrrolidine **9** (70 mg, 0.092 mmol) was suspended in freshly distilled CH_2Cl_2 and DMAP (50 mg, 0.41 mmol) and pyridine (0.3 mL) added. The mixture was stirred for 10 min at room temperature, and oxalyl acid monobenzyl ester monochloride (100 mg, 0.50 mmol) was added, and the mixture left to stir at room temperature for 2 h. The solvent was removed, the resulting residue dissolved in CS_2 (10 mL) and filtered to remove insoluble materials. The filtrate was then concentrated and purified by column chromatography (silica gel, toluene) to afford the product which was washed with MeOH (40 mL) and petroleum ether (40 mL) and dried in vacuum to give compound **11** as black powder (58 mg, 68%). ^1H NMR (400 MHz, 297 K, $\text{CDCl}_3/\text{CS}_2$, δ , ppm) 7.47 (d, $J = 6.3$ Hz, 2H), 7.35 (m, 3H), 5.51 (s, 2H), 5.45 (s, 4H); ^{13}C NMR (125 MHz, 297 K, $\text{CDCl}_3/\text{CS}_2$, δ , ppm) 160.85 (C=O), 157.49 (C=O), 153.01, 152.57, 147.50, 147.44, 146.49, 146.44, 146.26, 146.24, 145.80, 145.76, 145.61, 145.46, 145.45, 145.43, 145.31, 144.62, 144.51, 143.22, 142.83, 142.82, 142.25, 142.18, 142.10, 142.03, 140.46, 140.32, 137.51, 136.25, 135.94, 134.60, 129.15, 128.99, 128.96, 128.66, 128.44, 128.42, 125.53 (sp^2 carbons, 37 environments), 70.67, 69.09, 67.99, 59.35, 57.16 (sp^3 carbons, 5 environments); MALDI-TOF MS (DCTB/MeCN, m/z): 924.1 (M^-); IR (KBr, ν , cm^{-1}): 2924 (m), 2362 (m), 1718 (s, C=O), 1671 (s, C=O), 1438 (m), 1125 (s), 527 (s).

Synthesis of 12

Compound **11** (5 mg) was dissolved in freshly distilled CH_2Cl_2 (5 mL), and $\text{CF}_3\text{SO}_3\text{H}$ (0.05 mL) added. The resulting mixture was stirred for 1 h at room temperature after which the solvent was removed under vacuum and the resultant brown solid was suspended in diethyl ether (10 mL). The precipitate was separated by centrifugation, the ether removed by decantation, and this procedure was repeated three times. The resultant brown solid was dried under vacuum to give the product, **12** (4 mg, 95%) as a brown solid. MALDI-TOF MS (DCTB/MeCN, m/z): 791.2 (M^-); IR (KBr, ν , cm^{-1}): 3446 (s, NH), 2964 (m), 2360 (m), 1636 (s, C=O), 1507 (m), 1384 (s), 1216 (m), 527 (m).

Synthesis of 13 [24]

NaI (5.3 g, 34 mmol) was suspended in acetone (15 mL) and heated under reflux for 5 min. The mixture was cooled to room temperature, and benzyl bromoacetate (1 mL, 6.3 mmol) added. The reaction mixture was stirred at room temperature for 2 h and the solvent removed under vacuum. The resulting mixture was partitioned between water (20 mL) and ethyl acetate (10 mL). The organic fraction was separated, washed with a saturated solution of $\text{Na}_2\text{S}_2\text{O}_3$ (2×10 mL) followed by brine (10 mL) and dried over Na_2SO_4 . The solvent was removed to give the product (1.57 g, 90%) as a yellow oil; ^1H NMR

(300 MHz, 297 K, CDCl₃, δ , ppm) 7.40 (s, 5H), 5.20 (s, 2H), 3.76 (s, 2H); ¹³C NMR (75 MHz, 297 K, CDCl₃, δ , ppm) 168.60 (C=O), 135.14, 128.65, 128.54, 128.33, 67.81 (-CH₂-O-), -5.51 (-CH₂I); ESIMS (MeOH, *m/z*): 298.95 (M + Na)⁺.

Synthesis of 14

To a solution of [60]fulleropyrrolidine **9** (110 mg, 0.144 mmol) in dry DMF (30 mL) benzyliodoacetate (150 mg) was added, and the resulting mixture heated to 100 °C for 1 h. The solvent was then removed under vacuum, and the resulting solid purified by column chromatography (silica gel, eluted with CS₂, followed by CS₂/toluene 1:1 v/v). The product was washed with MeOH (40 mL) and the resultant solid was dried in vacuum to give compound **14** as a black powder (80 mg, 61%). ¹H NMR (400 MHz, 297 K, CDCl₃/CS₂, δ , ppm) 7.49 (d, *J* = 6.8 Hz, 2H), 7.42 (m, 3H), 5.37 (s, 2H), 4.68 (s, 2H), 4.09 (s, 2H); ¹³C NMR (125 MHz, 297 K, CDCl₃/CS₂, δ , ppm) 169.31 (C=O), 154.61, 147.37, 146.33, 146.14, 146.03, 145.74, 145.56, 145.36, 144.62, 143.18, 142.72, 142.28, 142.16, 141.98, 140.26, 136.39, 135.64, 135.22, 128.81, 128.62, 128.53, 128.37 (sp² carbons, 22 environments), 70.58, 67.05, 66.78, 54.84 (sp³ carbons, 4 environments); MALDI-TOF MS (DCTB/MeCN *m/z*): 911.5 (M⁻); IR (KBr, ν , cm⁻¹): 2962 (w), 2359 (w), 1736 (s, C=O), 1393 (m), 1344 (m), 1095 (s), 737 (m), 527 (s).

Synthesis of 15

To a solution of **14** (5 mg, 0.0055 mmol) in dry CH₂Cl₂ (5 mL) CF₃SO₃H (0.05 mL) was added and the mixture was stirred for 2 h at room temperature. The solvent was removed under vacuum and the resultant brown solid suspended in diethyl ether (10 mL). The precipitate was separated by centrifugation, the ether removed, and this procedure was repeated three times. The resultant brown solid was dried in vacuum to give the product, **15** (4.2 mg, 90%); MALDI-TOF MS (DCTB/MeCN, *m/z*): 821.2 (M⁻); IR (KBr, ν , cm⁻¹): 3446 (s, OH), 2957 (w), 2361 (w), 1732 (m, C=O), 1483 (m), 1170 (m), 746 (m), 527 (s).

Supporting Information

Supporting Information File 1

Additional spectra.

[<http://www.beilstein-journals.org/bjoc/content/supplementary/1860-5397-10-31-S1.pdf>]

Acknowledgements

We thank the European Research Council, the EPSRC, the Royal Society and the University of Nottingham for financial support of this work.

References

- Popov, A.; Yang, S.; Dunsch, L. *Chem. Rev.* **2013**, *113*, 5989–6113. doi:10.1021/cr300297r
- Hameit, W. *Phys. Rev. A* **2002**, *65*, 032322. doi:10.1103/PhysRevA.65.032322
- Ardavan, A.; Blundell, S. J. *J. Mater. Chem.* **2009**, *19*, 1754–1760. doi:10.1039/b809525f
- Liu, G.; Khlobystov, A. N.; Charalambidis, G.; Coutsolelos, A. G.; Briggs, G. A. D.; Porfyrakis, K. *J. Am. Chem. Soc.* **2012**, *134*, 1938–1941. doi:10.1021/ja209763u
- Farrington, B. J.; Jevric, M.; Rance, G. A.; Ardavan, A.; Khlobystov, A. N.; Briggs, G. A. D.; Porfyrakis, K. *Angew. Chem., Int. Ed.* **2012**, *51*, 3587–3590. doi:10.1002/anie.201107490
- Hörmann, F.; Hirsch, A.; Porfyrakis, K.; Briggs, G. A. D. *Eur. J. Org. Chem.* **2011**, 117–121. doi:10.1002/ejoc.201000867
- Plant, S. R.; Jevric, M.; Morton, J. J. L.; Ardavan, A.; Khlobystov, A. N.; Briggs, G. A. D.; Porfyrakis, K. *Chem. Sci.* **2013**, *4*, 2971–2975. doi:10.1039/c3sc50395j
- Kanai, M.; Porfyrakis, K.; Briggs, G. A. D.; Dennis, T. J. S. *Chem. Commun.* **2004**, 210–211. doi:10.1039/b310979h
- Echegoyen, L.; Echegoyen, L. E. *Acc. Chem. Res.* **1998**, *31*, 593–601. doi:10.1021/ar970138v
- Chamberlain, T. W.; Davies, E. S.; Khlobystov, A. N.; Champness, N. R. *Chem.–Eur. J.* **2011**, *17*, 3759–3767. doi:10.1002/chem.201003092
- Segura, J. L.; Martín, N. *Chem. Soc. Rev.* **2000**, *29*, 13–25. doi:10.1039/a903716k
- Komatsu, K.; Wang, G.-W.; Murata, Y.; Tanaka, T.; Fujiwara, K.; Yamamoto, K.; Saunders, M. *J. Org. Chem.* **1998**, *63*, 9358–9366. doi:10.1021/jo981319t
- Lebedev, S.; Ballenweg, S.; Gross, J.; Taylor, R.; Krätschmer, W. *Tetrahedron Lett.* **1995**, *36*, 4971–4974. doi:10.1016/0040-4039(95)00784-A
- Jin, X.; Xie, X.; Tang, K. *Chem. Commun.* **2002**, 750–751. doi:10.1039/b200793b
- Sánchez, L.; Herranz, M. Á.; Martín, N. *J. Mater. Chem.* **2005**, *15*, 1409–1421. doi:10.1039/b417580h
- Sastre-Santos, A.; Parejo, C.; Martín-Gomis, L.; Ohkubo, K.; Fernández-Lázaro, F.; Fukuzumi, S. *J. Mater. Chem.* **2011**, *21*, 1509–1515. doi:10.1039/c0jm02635b
- Gerson, F.; Huber, W. *Electron Spin Resonance Spectroscopy of Organic Radicals*; Wiley-VCH: Weinheim, 2003. doi:10.1002/3527601627
- Chamberlain, T. W.; Pfeiffer, R.; Peterlik, H.; Kuzmany, H.; Zerbetto, F.; Melle-Franco, M.; Staddon, L.; Champness, N. R.; Briggs, G. A. D.; Khlobystov, A. N. *Small* **2008**, *4*, 2262–2270. doi:10.1002/sml.200800552
- de Lucas, A. I.; Martín, N.; Sánchez, L.; Seoane, C. *Tetrahedron Lett.* **1996**, *37*, 9391–9394. doi:10.1016/S0040-4039(97)82972-3
- Lebedeva, M. A.; Chamberlain, T. W.; Schröder, M.; Khlobystov, A. N. *Tetrahedron* **2012**, *68*, 4976–4985. doi:10.1016/j.tet.2012.04.061
- Maggini, M.; Scorrano, G.; Prato, M. *J. Am. Chem. Soc.* **1993**, *115*, 9798–9799. doi:10.1021/ja00074a056
- Duan, H.-F.; Xie, J.-H.; Qiao, X.-C.; Wang, L.-X.; Zhou, Q.-L. *Angew. Chem., Int. Ed.* **2008**, *47*, 4351–4353. doi:10.1002/anie.200800423
- Wallach, L.; Lehmann, F. *Justus Liebigs Ann. Chem.* **1887**, 237, 236–260. doi:10.1002/jlac.18872370205

24. Wagner, R.; Rhoades, T. A.; Or, Y. S.; Lane, B. C.; Hsieh, G.; Mollison, K. W.; Luly, J. R. *J. Med. Chem.* **1998**, *41*, 1764–1776. doi:10.1021/jm960066y
25. Balch, A. L.; Costa, D. A.; Fawcett, W. R.; Winkler, K. *J. Phys. Chem.* **1996**, *100*, 4823–4827. doi:10.1021/jp953144m
26. Lee, K.; Song, H.; Kim, B.; Park, J. T.; Park, S.; Choi, M.-G. *J. Am. Chem. Soc.* **2002**, *124*, 2872–2873. doi:10.1021/ja017496k
27. Zanello, P.; de Biani, F. F.; Cinquantini, A.; Grigiotti, E. *C. R. Chim.* **2005**, *8*, 1655–1659. doi:10.1016/j.crci.2005.03.011
28. Brustolon, M.; Zoleo, A.; Agostini, G.; Maggini, M. *J. Phys. Chem. A* **1998**, *102*, 6331–6339. doi:10.1021/jp981385z
29. Sun, Y.; Drovetskaya, T.; Bolskar, R. D.; Bau, R.; Boyd, P. D. W.; Reed, C. A. *J. Org. Chem.* **1997**, *62*, 3642–3649. doi:10.1021/jo970357u
30. Dubois, D.; Jones, M. T.; Kadish, K. M. *J. Am. Chem. Soc.* **1992**, *114*, 6446–6451. doi:10.1021/ja00042a023
31. Mori, N.; Fukui, K.; Nakazawa, S.; Takekuma, S.; Takekuma, H.; Yoshida, Z.; Sato, K.; Shiomi, D.; Takui, T. *Synth. Met.* **2003**, *137*, 1315–1316. doi:10.1016/S0379-6779(02)01003-2

License and Terms

This is an Open Access article under the terms of the Creative Commons Attribution License (<http://creativecommons.org/licenses/by/2.0>), which permits unrestricted use, distribution, and reproduction in any medium, provided the original work is properly cited.

The license is subject to the *Beilstein Journal of Organic Chemistry* terms and conditions: (<http://www.beilstein-journals.org/bjoc>)

The definitive version of this article is the electronic one which can be found at:
[doi:10.3762/bjoc.10.31](https://doi.org/10.3762/bjoc.10.31)